Available online at www.sciencedirect.com
ScienceDirect
European Journal of Pharmaceutics and Biopharmaceutics 69 (2008) 31–42
European Journal of Pharmaceutics and Biopharmaceutics
www.elsevier.com/locate/ejpb

Research paper

Charged nanoparticles as protein delivery systems: A feasibility study using lysozyme as model protein

Cuifang Cai [a,b], Udo Bakowsky [a], Erik Rytting [a], Andreas K. Schaper [c], Thomas Kissel [a,*]

[a] Department of Pharmaceutics and Biopharmacy, Philipps Universität of Marburg, Marburg, Germany
[b] School of Pharmacy, Shenyang Pharmaceutical University, Shenyang, China
[c] Department of Geosciences and Materials Science Center, Philipps Universität of Marburg, Marburg, Germany

Received 4 July 2007; accepted in revised form 8 October 2007
Available online 12 October 2007

Abstract

The aim of this study was to investigate the feasibility of negatively charged nano-carriers (nanoparticles), consisting of polymer blends of poly(lactide-co-glycolide) (PLGA) and poly(styrene-co-4-styrene-sulfonate) (PSS), to improve the loading capacity and release properties of a positively charged model protein, lysozyme, through an adsorption process. Nanoparticles were prepared by a solvent displacement method and characterized in terms of size, ζ-potential, morphology, as well as loading capacity of model protein lysozyme. Morphology of these particles was investigated using transmission electron microscopy (TEM), scanning electron microscopy (SEM) and atomic force microscopy (AFM). The loading capacity of lysozyme was evaluated as a function of polymer blend ratio, protein concentration, pH, and ionic strength; in vitro release profiles were also studied. The results show that negatively charged nanoparticles were obtained using polymer blends of PLGA and PSS, characterized by increased net negative surface charge with increasing ratios of PSS. Moreover, protein loading capacity increased as function of PSS/PLGA ratio. Increased pH facilitated the adsorption process and improved the loading capacity. Maximum loading efficiency was achieved at salt concentrations of 50 mM. In vitro release of lysozyme from the polymer blend nanoparticles was dependent on drug loading and full bioactivity of lysozyme was preserved throughout the process. These findings suggest that this is a feasible method to prepare nanoparticles with high surface charge density to efficiently adsorb oppositely charged protein through electrostatic interactions.

Keywords: Charged nanoparticles; Lysozyme; Electrostatic interaction; Protein delivery; Charge density

1. Introduction

Recent years have seen increasing interest in polymeric nanoparticles as carriers for hydrophilic macromolecules such as proteins, vaccines, and polynucleotides [1,2]. Numerous investigations have shown that nanoparticles can not only improve the stability of therapeutic agents against enzymatic degradation and control the release of therapeutic agents, but they can also be delivered to distant target sites either by localized delivery using a catheter-based approach with a minimal invasive procedure, or they can be conjugated to a biospecific ligand which could direct them to the target tissue or organ [1,3]. For an effective nanoparticulate delivery system, the nanoparticle size and loading must be adjusted carefully, and protein stability during preparation and release must be ensured. Depending on the preparation method, drugs or antigens can either be entrapped in the polymer matrix, encapsulated in a liquid core, surrounded by a shell-like polymer membrane, or bound to the particle surface by adsorption [4]. Some reported methods for preparing nanoparticles from

* Corresponding author. Department of Pharmaceutics and Biopharmacy, Philipps Universität of Marburg, Ketzerbach 63, D-35032 Marburg, Germany. Tel.: +49 6421 282 5881; fax: +49 6421 282 7016.
E-mail address: kissel@staff.uni-marburg.de (T. Kissel).

0939-6411/$ - see front matter © 2007 Elsevier B.V. All rights reserved.
doi:10.1016/j.ejpb.2007.10.005

biodegradable polymers include: emulsification solvent evaporation [5], emulsion polymerization [6], salting out procedure [7], and nanoprecipitation [8].

The w/o/w double emulsion technique has been widely used for protein micro- and nano-encapsulation. Unfortunately, this method requires high shear forces and organic solvent, both of which are usually detrimental to proteins. Solvent displacement has become a popular alternative for this purpose. This technique does not rely on shear stress to produce nanoparticles, but takes advantage of differences in the interfacial tension, a phenomenon also designated as the Marangoni effect [9,10]. However, the use of this technique may still expose the protein to organic solvent during nanoparticle preparation or to high acidity if the release of the protein does not outpace the polymer degradation [11]. Moreover, the solvent displacement method typically results in low encapsulation efficiency for water soluble drugs [12]. Thus, a method to associate the protein to the preformed nanoparticle surface by adsorption has been investigated [13]. This technique can be performed in an aqueous solution and at a low temperature, thus improving the prospects for preserved activity of sensitive drug molecules.

However, a successful nanoparticle system should have a high loading capacity to reduce the dose of the carrier required for administration. As previously reported, lower loading efficiency was observed for the adsorption process compared to the encapsulation method, and the capacity of adsorption is related to the hydrophobicity of the polymer and the specific area of the nanoparticles [2]. As to the protein adsorption process, both Coulomb (electrostatic) and van der Waals interactions (hydrophobic) are thought to be governing factors for the adsorption of proteins. However, the hydrophobic nature of polymer results in the denaturation and aggregation of proteins [14,15]. This highlights the importance of electrostatic interactions in the process of protein adsorption. The fundamental electrostatic interactions between particles and proteins have not been fully investigated so far, and little is known about the particle properties that are critical to adsorption efficiency and the protein bioactivity [16].

Based on these considerations, we have undertaken this work to explore the potential of negatively charged nanoparticles as a delivery vehicle for positively charged proteins, with the goal to attain a high level of protein loading with full bioactivity. Negatively charged sulfobutylated branched polyesters SB-PVA-g-PLGA were successfully used for nanoparticle preparation and protein adsorption with tetanus toxoid [4,17]. In order to guide further modification of this polymer, investigations regarding the influence of charge density on nanoparticle properties and protein interactions are of importance. For this purpose, PSS, a partially sulfonated polystyrene containing sulfonic acid groups attached to the backbone, was selected to modify the charge density of PLGA nanoparticles, intended to prepare nanoparticles of varying negative charge density. Lysozyme, a 14.3 kDa basic protein with a high isoelectric point (p$I \approx 11$), was employed in this study as a model positively charged protein because of its detailed characterization and the straightforward assessment of its biological activity [18].

The first aim of this study was to establish the model consisting of negatively charged nanocarriers with variable charge density, prepared from a blend of PLGA and PSS using a solvent displacement method. The second step was to test the hypothesis that this strategy would result in improved loading efficiency and bioactivity preservation for adsorbed lysozyme. Finally, changes in pH and ionic strength were investigated to gain insight into the surface–protein and protein–protein electrostatic interactions.

2. Materials and methods

2.1. Materials

Poly(lactic-co-glycolic acid) (PLGA Resomer® RG502H) was supplied by Boehringer Ingelheim (Germany). Poly(styrene-co-4-styrene-sulfonate) (PSS, Parent polystyrene Mn = 133 200, Mw/Mn = 1.04, Sulfonation Degree: 50 mol% by Titration, Mn = 184,400, Mw = 191,800) was purchased from Polymer Source, Inc. (Dorval, Canada). The Micro BCA protein assay kit was from Pierce Chemical (Bonn, Germany). Hen egg white lysozyme, *Micrococcus lysodeikticus*, and cytochrome *C* from bovine heart (12,327 kDa, p*I* 10) were obtained from Sigma–Aldrich Chemie GmbH (Germany). Bovine serum albumin (BSA, 66.4 kDa, p*I* 4.7) was purchased from Hoechst Behring (Marburg, Germany). All other chemicals were purchased from Sigma, of analytical grade, and used without further purification.

2.2. Preparation of PLGA/PSS nanoparticles

Nanoparticles were prepared by a solvent displacement technique, as described previously [4,13]. Briefly, 10.0 mg of polymer at different mass ratios of PSS to PLGA (RG502H) was dissolved in 1 ml of acetone at 25 °C. The resulting solution was subsequently injected to a magnetically stirred (500 rpm) 5 ml aqueous phase of filter double distilled water (pH 7.0, conductance 0.055 μs/cm, 25 °C) using an electronic injection pump to inject the organic solution into the aqueous phase through an injection needle (Sterican 0.55 × 25 mm) at a constant flow rate (10.0 ml/min). After the injection of the organic phase the resulting colloidal suspension was stirred for 8 h under reduced pressure to remove the organic solvents. Particles were characterized and used directly after the preparation.

2.3. Physicochemical and morphological characterization of negatively charged nanoparticles

2.3.1. Particle size and ζ-potential measurements

The average particle size and ζ-potential of the nanoparticles were measured using a Zetasizer Nano ZS/ZEN3600

(Malvern Instruments, Malvern, UK). Particle size and polydispersity were determined using non-invasive back scatter (NIBS) technology, which allows sample measurement in the range of 0.6 nm–6 μm. Freshly prepared particle suspensions (800 μl) were placed in a folded capillary cell without dilution. The measurement was carried out using a 4 mW He–Ne laser (633 nm) as light source at a fixed angle of 173°. The following parameters were used for experiments: medium refractive index 1.330, medium viscosity 0.88 mPa s, dielectric constant 78.54, temperature 25 °C. Each size measurement included at least 10 runs. All measurements were carried out in triplicate, and the results were expressed as the mean size ± SD.

ζ-Potential was measured with a combination of laser Doppler velocimetry and phase analysis light scattering (PALS). A Smoluchowsky constant $F(K_a)$ of 1.5 was used to calculate ζ-potential values from the electrophoretic mobility. All measurements were carried out at 25 °C in triplicate, and the results were expressed as means ± SD.

2.3.2. Scanning electron microscopy (SEM)

Prior to SEM observation, nanoparticle suspensions were diluted 1/5 with ultrapure water, and a drop of diluted suspension was then directly deposited on a polished aluminum sample holder. Samples were dried in vacuo and subsequently sputter-coated with a carbon layer at 4–6 amps for 30 s then with a gold layer at 2 amps for 30 s at 5×10^{-5} Pa (Edwards Auto 306 Vacuum Coater, Edwards, Germany). Subsequently, the morphology of nanoparticles was observed at 3 kV using a scanning electron microscope (SEM, S-4200, Hitachi, Japan).

2.3.3. Transmission electron microscopy (TEM)

The samples were prepared by coating a copper grid (200 mesh covered with Formvar/carbon) with a thin layer of diluted particle suspension. After negative staining with 2% (w/v) phosphotungstic acid for 2 min, the copper grid was then dried at room temperature before measurement. Nanoparticles were investigated using transmission electron microscopy (TEM, Zeiss EM 10) at an accelerating voltage of 300 kV.

2.3.4. Atomic force microscopy (AFM)

To obtain information about the substructure and morphology of nanoparticles, AFM measurements were carried out in air under normal atmospheric conditions, using a NanoWizard (JPK Instruments, Berlin, Germany). Imaging was performed in contact mode using force in the range of 1–10 nN with pyramidal silicon nitride tips mounted on cantilevers of spring constant 0.036 Nm^{-1}. Height measurements and surface roughness were obtained using NanoWizard AFM image analysis software (JPK Instruments, version 2.1).

2.3.5. Differential scanning calorimetry (DSC)

Polymer films cast from 10% (w/v) acetone solutions on Teflon® plates were allowed to dry for 24 h under reduced pressure. Residual solvents were then removed in vacuo at room temperature until constant weights were obtained. Differential scanning calorimetry (DSC) was conducted under a nitrogen atmosphere using a DSC7 calorimeter (Perkin-Elmer) in sealed aluminum pans, relative to indium and gallium standards. Thermograms covered a range of −20 to 200 °C with heating and cooling rates of 10 °C/min. Glass transition temperatures (T_g) were determined from the second run.

2.4. Loading capacity of PLGA/PSS nanoparticles for lysozyme

Nanoparticle suspensions of defined concentrations were incubated with defined amounts of lysozyme for 5 h at 4 °C. The amount of adsorbed protein on the nanoparticles was calculated by measuring the difference between the amount of protein added to the nanoparticle solution and the measured non-entrapped protein remaining in the aqueous phase. After incubation, samples were centrifuged for 30 min at 13,000 rpm (25 °C), and the supernatant was checked for the non-bound protein by bicinchoninic acid (BCA) assay with measurement at 570 nm. For each protein concentration, a control tube was prepared without any nanoparticles to account for any protein loss due to adsorption to the Eppendorf tubes. Especially, for investigations with cytochrome *C* and bovine serum albumin (BSA), one-milliliter portions of nanoparticle suspension (1 mg/ml) were incubated with defined amounts of protein at 4 °C for 5 h in pH 7.0 PBS buffer (15 mM). Protein loading efficiency was calculated as follows:

$$\text{Protein loading efficiency} = \frac{\text{Total amount of protein} - \text{Free protein}}{\text{Total amount of protein}} \times 100\%$$

2.5. In vitro release of lysozyme from nanoparticles

For the release studies, protein loaded nanoparticles were stirred in 8 ml PBS buffer (pH 7.4) containing 0.05% NaN_3 and 0.01% Tween® 80 by vertical rotation at 37 °C with final concentration of nanoparticles at 1 mg/ml. At predetermined intervals, 1 ml aliquots were withdrawn and centrifuged (13,000 rpm, 30 min), after which the total protein content in the supernatant was determined by the BCA assay. All experiments were performed in triplicate.

2.6. In vitro bioactivity of lysozyme

Lysozyme activity was determined using the decrease in optical density at 450 nm of a *M. luteus* (*lysodeikticus*) suspension. Briefly, a 2.5 ml aliquot of *M. lysodeikticus* cell suspension (0.24 mg/ml in 66 mM PBS, pH 6.24) was incubated with either 50 μl of aqueous lysozyme solutions

obtained from the nanoparticles during the *in vitro* protein release tests or with lysozyme standard solutions (1–100 μl). The decrease in absorbance at 450 nm over time was related to the bioactivity of the lysozyme against the *M. lysodeikticus* cells. The relative bioactivity of lysozyme was calculated from the slope of the linear part of the curve (absorbance versus time) according to the technique described by van de Weert et al. [19].

2.7. Statistical analysis

Results are presented as means ± SD from at least three measurements. Significance between the mean values was calculated using ANOVA one-way analysis (Origin 7.0 SRO, Northampton, MA, USA). Differences were considered to be statistically significant at a level of $p \leqslant 0.05$.

3. Results and discussion

3.1. Solubility of PSS and compatibility of PSS/PLGA

The purpose of this work was to investigate the interaction between oppositely charged nanoparticles and proteins. With this concept in mind, the negative charge density of nanoparticles was varied by adding different amount of PSS in the polymer matrix. The solvent displacement technique was chosen to prepare nanoparticles because of narrow size distributions and the ability to prepare particles without the use of high shear stress and surfactants [4].

3.1.1. Solubility of PSS in organic solvent and aqueous phase

Solvent displacement is based on the precipitation of a dissolved polymer in solution upon addition to a miscible, surfactant-containing or free solution which is a non-solvent for the polymer [4]. Using this technique, organic solvents, such as acetone, dimethyl sulfoxide (DMSO), tetrahydrofuran (THF), and ethanol, are frequently used to dissolve the polymer; Poloxamer- or PVA-containing aqueous phases are commonly employed as the non-solvent.

The solubility of PSS was investigated at room temperature in different organic solvents and in acetate buffer at different pH values. PSS was totally dissolved in acetone, ethanol, and DMSO at 20 mg/ml. In the case of THF and dichloromethane, however, 5 mg/ml PSS was insoluble even after incubation at 37 °C between 24 and 48 h. The solubility of PSS in acetone at room temperature was determined to be 0.53 ± 0.01 g/ml.

PSS swelled and formed transparent polymer gel with greatly increased volume after 24 h incubation in acetate buffer of pH 3–12. A clear solution was observed at pH 2.26 at the concentration of 10 mg/ml. Based on these results, it could be concluded that it is feasible to prepare PLGA/PSS nanoparticles with solvent displacement in a wide pH range.

3.1.2. Compatibility of PSS and PLGA

PLGA and PSS were chosen in this work to mimic a charged polymer for preparation of nanoparticles of varying charge density. Both polymers were co-dissolved in organic solvent, and upon diffusion of the organic phase into water, both polymers formed nanoparticles. In order to verify that no phase separation occurred and that a homogeneous polymer blend structure is formed during the aggregation process, DSC experiments were carried out to investigate the compatibility of PLGA and PSS.

Different ratios of these polymers were dissolved in acetone and polymer blend films were prepared after evaporation of organic solvent. DSC experiments were performed for polymer blend films and placebo nanoparticles. For all samples, only one T_g was observed in the thermogram, indicating that no phase separation occurred and a homogeneous polymer blend was obtained. The T_g of pure PLGA (RG502H) is 42.23 °C, and when the ratio of PSS in the polymer blend increased, Fig. 1 shows that the T_g gradually decreased, to 34.14 °C at 80% PSS, even though the T_g of pure PSS is much higher (156.34 °C). In the case of placebo nanoparticles, a decrease in Tg from 44 to 39 °C was observed with the increase of PSS from 0% to 10%, which is in agreement with the observations of the polymer blend films. These results demonstrate the homogeneous

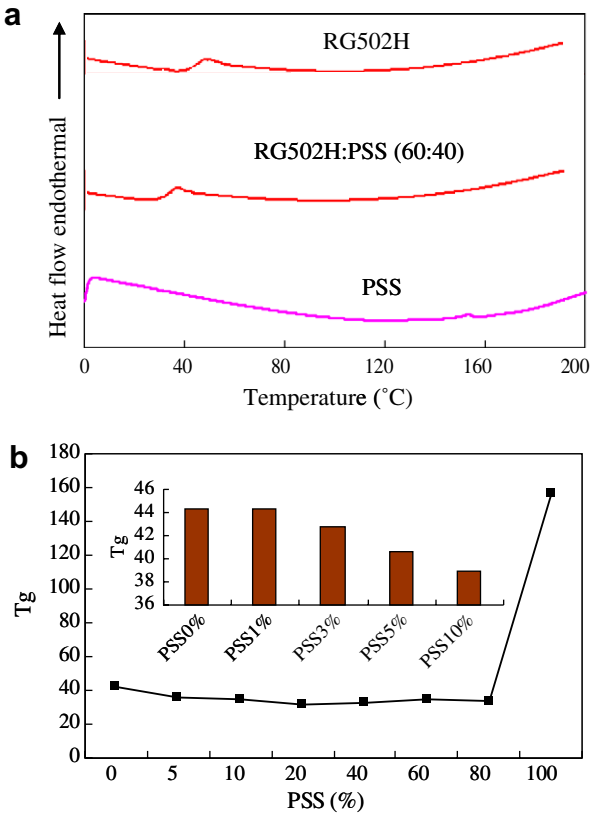

Fig. 1. (a) DSC scans of polymer PLGA (RG502H), PSS, and polymer blend PLGA/PSS. (b) Glass transition temperature (T_g) of polymer blend films with varied amount of PSS. The inset shows the T_g of nanoparticles with different amount of PSS.

structure of polymer blends from PLGA and PSS, and the decrease in T_g indicated the possible interaction of PSS and PLGA.

3.2. Characterization of PLGA/PSS blend nanoparticles

Nanoparticles were prepared with a polymer blend of PSS and PLGA at different mass ratios, following the same standard preparation protocol in order to exclude any influence of technological aspects. Preliminary experiments showed that high amounts of PSS (20%, 30%) led to much higher increased particle size (>300 nm) and larger polydispersity (>0.4), and a plateau in the ζ-potential, which could be attributed to the swelling of PSS in water and saturation of functional groups on the nanoparticle surface. Therefore, in order to investigate the variable charge density of nanocarriers with minimal influence of swelling or increased particle size, polymer blend nanoparticles were examined at ratios of PSS to PLGA between 0% and 10%.

The particle size, polydispersity index, and ζ-potential values of the nanoparticles in this range are presented in Table 1. The size and ζ-potential were significantly influenced by blending PLGA with PSS. A mass ratio of 10% PSS to PLGA resulted in an increase in the mean particle size from 122 to 200 nm as a consequence of PSS swelling in water. The polydispersity index was less than 0.25 in all cases, indicating narrow size distributions.

As expected, the ζ-potential decreased with increasing amounts of PSS. The sulfonic acid functional groups modified the charge density of nanoparticles characterized with strongly increased negative charge upon addition of PSS (to <-50 mV). The pH of nanoparticle suspensions decreased from pH 6.5 for pure PLGA to pH 4.2 for the polymer blend containing 10% PSS. The nanoparticles in the present study were found to be stable in dispersion state at room temperature for at least 24 h, even without using surfactant during the preparation process, due to the high absolute values of ζ-potential.

SEM and TEM images are shown in Fig. 2. In general, SEM micrographs revealed a compact and spherical structure independent of PLGA–PSS ratio, with a size distribution confirming the size measurements by PCS. TEM micrographs also demonstrated well-defined spherical particle morphologies, with a more stained outer layer that could be attributed to the orientation of PSS on the surface due to the hydrophilic property of the sulfonic acid groups. AFM images in Fig. 2 showed smooth nanoparticle surface without any noticeable pinholes or cracks.

Table 1
Characteristics of polymer blend nanoparticles prepared from different mass ratios (% PSS in PLGA), $n = 3$

Mass ratio PSS: RG502H (%)	Size (nm)	Polydispersity index (PdI)	ζ-Potential (mV)
0	122 ± 1.4	0.09 ± 0.01	−32.28 ± 1.77
1	143 ± 5.6	0.09 ± 0.01	−40.23 ± 2.37
3	165 ± 3.4	0.11 ± 0.02	−48.73 ± 0.61
5	180 ± 15.7	0.11 ± 0.02	−52.26 ± 1.92
10	200 ± 10.8	0.10 ± 0.03	−56.48 ± 0.26

3.3. Lysozyme loading capacity of the polymer blend nanoparticles

As mentioned previously, the primary aim of this study was to improve protein loading efficiency via electrostatic interactions. Nanoparticle surface charge density was modified successfully using PLGA and PSS polymer blends, and these nanoparticles were used to investigate the loading capacity of lysozyme, a model electropositive protein. The interactions of oppositely charged protein and nanoparticle were evaluated in terms of the particle size, ζ-potential, and loading efficiency.

3.3.1. Characteristics of protein loaded nanoparticles

A 1 mg/mL nanoparticle suspension (10% PSS) was incubated with different mass ratios of protein. After incubation with lysozyme solution, the nanoparticles were evaluated in terms of size, ζ-potential, and adsorption efficiency. Fig. 3 shows that the ζ-potential of polymer blend nanoparticles increased with increasing protein concentrations. Between 0% and 10% theoretical drug loading, a linear relationship was observed between protein concentration and ζ-potential ($R^2 = 0.999$). Further increases in lysozyme concentration led to sharply elevated ζ-potential up to the 40% mass ratio of lysozyme to nanoparticles. The plateau value around 35 mV indicates saturation of the particle surface. This reversal of surface charge from negative to positive confirms the adsorption of lysozyme to the nanoparticle surface.

Fig. 3 also shows that nanoparticle size increased linearly between 0% and 10% lysozyme ($R^2 = 0.994$). At the mass ratio of 20%, the ζ-potential is close to zero; obvious flocculation was observed due to the lack of charge stabilization and the size could not be measured. At higher protein concentrations as mass ratio of 40%, increased particles size as 242.7 nm was detected compared to 198.3 nm for placebo nanoparticles.

After protein loading at the 40% mass ratio, the SEM images in Fig. 2 still show well-defined nanoparticle structure similar to the placebo particles, and no aggregates were observed. Upon close observation of the TEM image, double layers were seen in the protein-loaded nanoparticles when the samples were treated with negative staining. The inner white region corresponds to the polymeric nanoparticle core, and the hydrophilic nanoparticle shell is colored dark grey. The outer layer shows the protein on the nanoparticle surface, and excess unbound protein appears in the stained background. The AFM image of the protein loaded particles reveals a slightly rougher surface than the blank particles.

The loading efficiency was dependent on lysozyme concentration. More specifically, at 50 μg/ml lysozyme (corresponding to a 5% mass ratio), the adsorption efficiency was

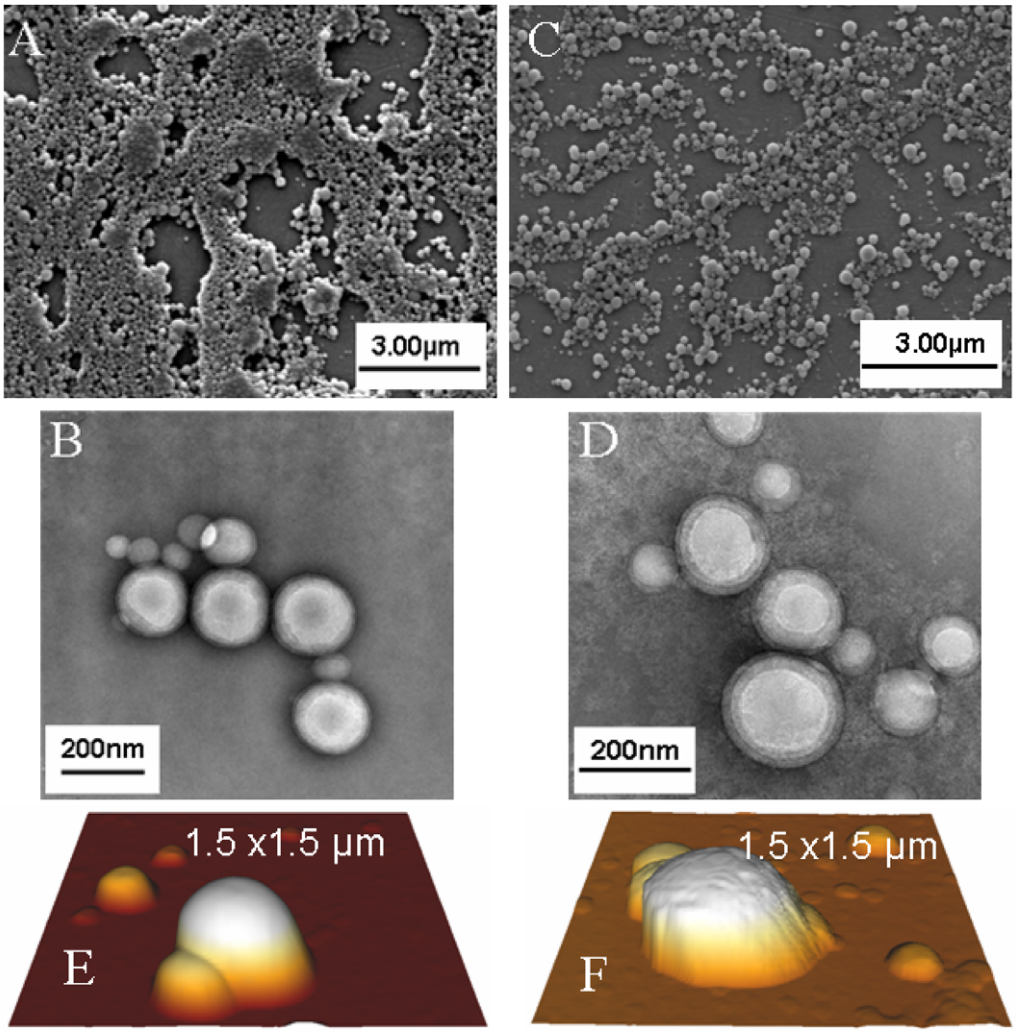

Fig. 2. Micrographs of placebo and lysozyme-loaded nanoparticles prepared from PLGA/PSS (10% PSS). (A) SEM, (B) TEM, (E) AFM for placebo nanoparticles, and (C) SEM, (D) TEM, (F) AFM for protein-loaded nanoparticles at 40% theoretical drug loading.

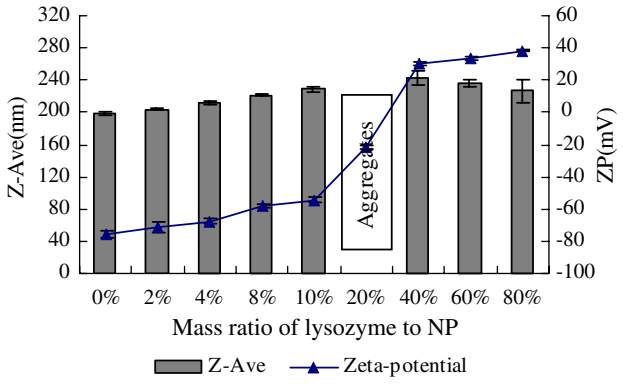

Fig. 3. Size (Z-Ave) and ζ-potential (ZP) of PLGA/PSS (10% PSS) nanoparticles after incubation with lysozyme at different concentrations. Error bars indicate the standard deviation ($n = 3$).

53%, but this value increased with increasing protein concentration, to a maximum of 100% loading efficiency at 250 μg/mL lysozyme (25% mass ratio). This increase in loading efficiency may be explained by the improved mobility of ions in the incubation medium and the slightly elevated ionic strength in the presence of protein molecules. In contrast, at lower concentration, electrostatic interaction as the driving force for this adsorption process is relatively weak due to the longer distance between protein and nanoparticles. Fig. 4 shows that for 10% PSS, at lysozyme concentrations above 250 μg/mL, the amount of protein adsorbed on the nanoparticle surface reached a plateau. Therefore, concentrations above this saturation point resulted in decreased loading efficiency.

3.3.2. Effect of polymer ratio of PSS to PLGA

Fig. 5 shows the ζ-potential values resulting from lysozyme loading at various mass ratios to nanoparticle suspensions prepared at different polymer ratios. As expected, the ζ-potential increased with increased drug loading in all cases, with maximum values between 30 and 40 mV. As the amount of PSS increased from 0% to 10%, the "isoelectric point" of the protein loaded nanopar-

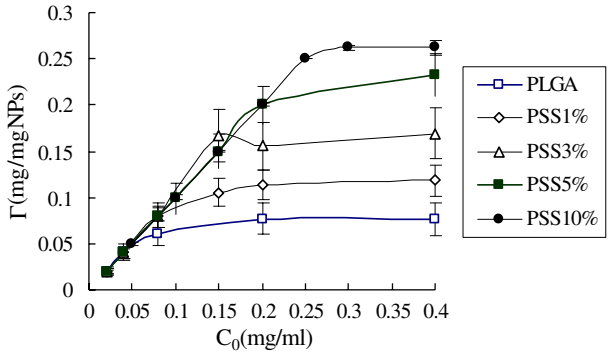

Fig. 4. Loading capacity (Γ) of PLGA/PSS nanoparticles at different mass ratios of PSS to PLGA for lysozyme after incubation with protein at different concentrations. Error bars indicate the standard deviation ($n = 3$).

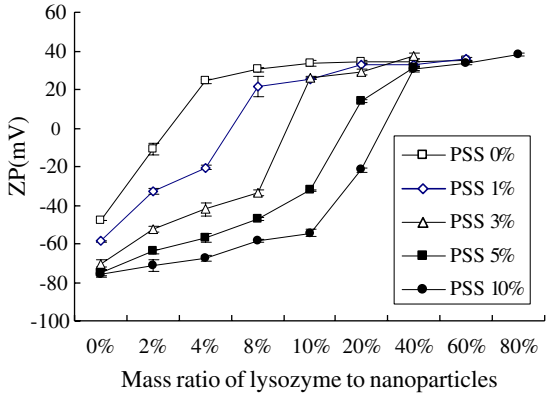

Fig. 5. ζ-Potentials (ZP) of PLGA/PSS nanoparticles at different mass ratios of PSS to PLGA after incubation with lysozyme at different concentrations. Values are given as means ± SD ($n = 3$).

ticles shifted from around 2% to 30% lysozyme (mass ratio). This suggests that increased amounts of PSS augmented the net negative charge on the surface of the nanoparticles, thus requiring larger amounts of positively charged lysozyme in order to neutralize the surface charge. In contrast, the ζ-potential of nanoparticles containing no PSS (pure RG502H) had already reversed to a positive value at a theoretical drug loading of only 4%.

The loading capacity of nanoparticles at different polymer ratios in Fig. 4 is remarkably high with these polymer blend nanoparticles, compared to reports of similar work. According to Jung et al. [13], the maximum amount of tetanus toxoid adsorbed onto nanoparticles prepared with the SB(43)-PVA-PLGA10 polymer is about 60 μg/mg nanoparticles. However, the polymer blend nanoparticles in this work have a loading capacity as high as 250 μg/mg nanoparticles. Increased amounts of PSS resulted in a higher loading capacity, as the increased density of charge-containing surfaces offers more potential binding sites for coulombic interactions with the protein molecules. The electrostatic properties of both the charged surface and the charged protein molecule play an important role in the overall protein adsorption process. This result is also in agreement with the findings of Wittemann et al. [20–25], in which spherical polyelectrolyte brushes (SPBs) can trap high amounts of protein within the brush. SPBs consist of solid polymer cores, poly(styrene), for example, onto which linear polyelectrolyte chains such as poly(styrene sulfonic acid) are grafted. Norde and Lyklema [26,27] also studied the adsorption behavior of HSA and bovine pancreas nuclease at negatively charged polystyrene surfaces using potentiometric titration, in which they postulated the formation of ion pairs between sulfate groups on the polystyrene surface and positively charged protein groups. In contrast, RG502H demonstrated comparatively low protein loading capacity; in this case, particle aggregates were observed in the nanoparticle suspension at a theoretical loading as low as 5%.

At steady state, the adsorbed amount of lysozyme Γ was established as a function of the lysozyme equilibrium concentration c_e, and an adsorption isotherm (Γ vs. c_e) was constructed. These lysozyme adsorption data were then fitted to the Langmuir equation expressed by Eq. (1), where Γ is the amount of adsorbed protein, c_e is the equilibrium protein concentration in the incubation medium, b is a coefficient related to the affinity between the nanoparticles and protein, and Q_0 is the maximum adsorption capacity.

$$\frac{c_e}{\Gamma} = \frac{1}{Q_0 b} + \frac{c_e}{Q_0} \quad (1)$$

The parameters for this equation appear in Table 2, where the linear regression analysis shows a good fit, with all correlation coefficients (R^2) greater than 0.999. The results indicate that under the conditions of this experiment, the protein adsorbs as a monolayer around the particles. Multilayer formation, as described by the Freundlich isotherm, was not observed even at higher protein concentrations, which is in accordance with previous work [13]. Moreover, the data fitted to the Langmuir model reflect the increased affinity (constant b) of the positively charged protein to the nanoparticle surfaces upon increased amounts of negatively charged sulfonic groups (PSS content). Chesko et al. also have reported that data for protein binding to anionic PLGA/DDS microparticles fit the Langmuir model, providing evidence that a monolayer of adsorbed protein is formed [28]. However, only when

Table 2
Langmuir equation parameters and free energy for the adsorption of lysozyme onto PLGA/PSS nanoparticles

Polymer	Q_0 (μg/mg nanoparticles)	b (ml/mg)	K_a	ΔG° (kJ/mol)	R^2
RG502H	77.5	0.276	21.41	−7.06	0.9998
PSS:PLGA 1%	119.1	0.301	35.84	−8.24	0.9996
PSS:PLGA 3%	172.4	0.433	74.63	−9.93	0.9997
PSS:PLGA 10%	250.0	0.851	212.76	−12.34	0.9995

Q_0, maximum adsorption capacity.
b, affinity constant of lysozyme for the nanoparticles.
K_a, equilibrium association constant, $K_a = Q_0 b$.
ΔG°, Gibbs free energy, $\Delta G^\circ = -RT\ln K_a$.

concentration of lysozyme is higher than that at which the maximum loading efficiency could be achieved, the adsorption follows the Langmuir isotherm. This is possibly due to the influence of lysozyme concentration on loading capacity. At lower lysozyme concentration, loading capacity is relatively lower due to the inefficient adsorption.

3.3.3. Effect of pH

Protein adsorption to hydrophobic polymers has frequently been investigated based on interactions between the hydrophobic domains of the protein and the hydrophobic polymer surface. Hydrophilic surfaces usually repel hydrophobic protein segments and decrease protein adsorption. In our study, however, the surface association between the negatively charged particles and the positively charged protein is hypothesized to be driven by the electrostatic interaction. In the incubation medium, both the particles and the protein surface charge are neutralized by counter ions. This affects the ζ-potential, which leads to charge redistribution and/or charge transfer between the polymeric surface and the protein molecule. To further investigate the adsorption mechanisms and to evaluate the important parameters in this adsorption process, the influence of pH in the incubation medium was studied.

Fig. 6 shows the ζ-potential profiles as a function of incubation medium pH for unloaded polymer blend nanoparticles. As expected, the ζ-potentials decreased at higher pH values due to the increasing dissociation of the sulfonic acid groups at the nanoparticle surface. The resulting increase in negative charge density on the nanoparticle surface at elevated pH supplied more binding sites for the positively charged protein. Upon summing up all charged amino acids and taking into account their dissociation ratios according to refs [29,30], the net positive charge of lysozyme decreases at higher pH, suggesting that more protein is required to neutralize the negatively charged nanoparticle surface. This leads to an increase in loading efficiency at higher pH, as seen in Fig. 6, from 65.5% at pH 4.52 to 100% at the higher pH values. These results suggest that electrostatic interactions dominate the adsorption process and that the surface charge density at a given pH governs the maximum amount of protein adsorbed.

3.3.4. Effect of ionic strength

As ionic strength can have a shielding effect on electrostatic forces, the influence of ionic strength on nanoparticles' properties and protein adsorption was studied by incubating the nanoparticles with various concentrations of NaCl. Fig. 7 shows that particle size was not influenced by ionic strength, and other than a jump in ζ-potential from −67 to −46 mV (at 0 and 1 mM), there was little change in ζ-potential at higher ionic strength values.

Fig. 8 shows that increases in ionic strength caused increased adsorption efficiency between 0 and 50 mM. At higher salt concentrations, a slight decrease in loading efficiency was observed. The trend was similar for both theoretical drug loading values (60% and 80%). In other words, maximum lysozyme adsorption was attained at a salt

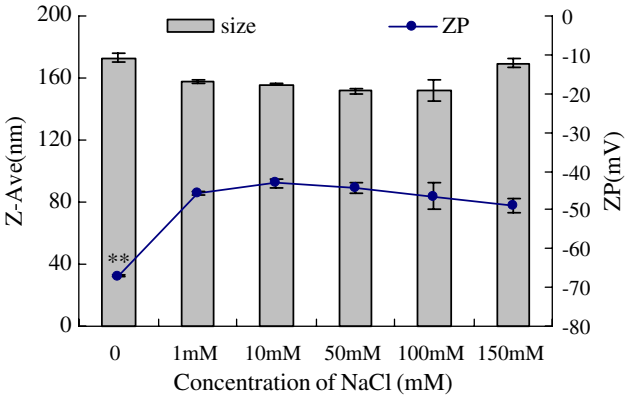

Fig. 7. Size (Z-Ave) and ζ-potential (ZP) of PLGA/PSS nanoparticles (10% PSS) at different salt concentrations. Error bars indicate the standard deviation ($n = 3$). $^{**}P < 0.01$ for ζ-potential at NaCl concentration of 0 mM compared to all other NaCl concentrations.

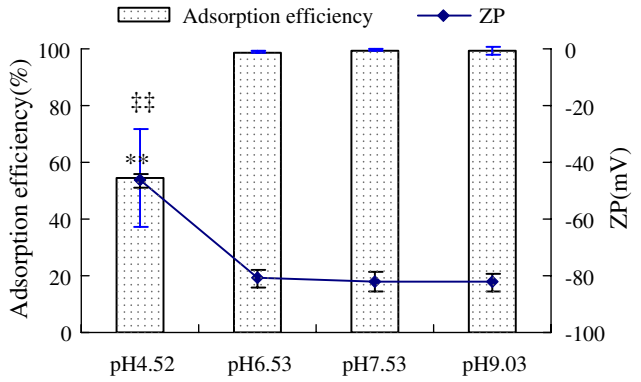

Fig. 6. ζ-Potentials (ZP) of PLGA/PSS (10% PSS) nanoparticles and adsorption efficiency of lysozyme at different pH values at 40% theoretical protein loading. Error bars indicate the standard deviation ($n = 3$). $P < 0.01$ ‡‡ for ζ-potential and ** for adsorption efficiency.

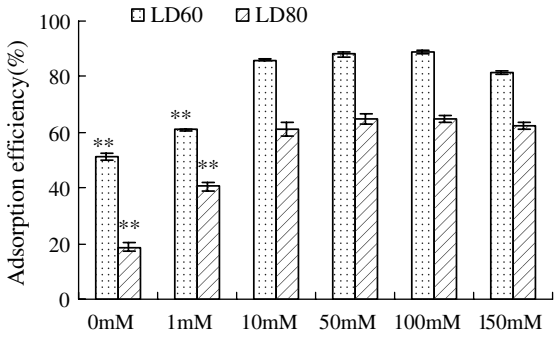

Fig. 8. Adsorption efficiency of protein on PLGA/PSS (10% PSS) nanoparticles as a function of salt concentration at theoretical drug loading of 60% (LD60) and 80% (LD80). Error bars indicate the standard deviation ($n = 3$). $^{**}P < 0.01$ for adsorption efficiency at NaCl concentration of 0 and 1 mM compared to other NaCl concentrations.

concentration of 50 mM. This observation indicates that in addition to electrostatic effects, hydrophobic interactions may still play a role in this adsorption process especially at lower ionic strength. It has been previously reported that increases in ionic strength could promote the hydrophobic interactions of dye molecules with a poly(GMA) surface [31]. Similarly, enhanced adsorption of negatively charged BSA to negatively charged planar surfaces composed of poly(styrene sulfonic acid) or silica is only observed at higher ionic strength [32]. Zhang et al. also reported maximum BSA adsorption at a salt concentration of 200 mM [33]. In summary, while electrostatic interactions play an important role in protein adsorption, hydrophobic interactions also contribute at lower ionic strength values.

3.4. Adsorption of BSA and cytochrome C

It has been clearly demonstrated that the higher negative charge density of nanoparticles favors loading of the electropositively charged model protein lysozyme. As part of this feasibility study, and to gain further insights into the process of protein adsorption to these PLGA/PSS nanoparticles, investigations were carried out using proteins with different properties. Cytochrome *C* (p*I* 10, Mw 12.3 kDa) was chosen as a protein with similar properties to lysozyme (p*I* 10.7, Mw 14.6 kDa), and BSA (bovine serum albumin) was chosen as a model negatively charged protein. BSA adsorption has been previously characterized by hydrophobic interactions with particles [32,33]. In addition to studies with the PLGA/PSS (10%) blend nanoparticles, the adsorption process was also compared to pure PLGA nanoparticles. These studies are important for understanding the interactions of nanoparticles and proteins, and their resulting applications for protein loading.

As seen in Fig. 9a and b, the surface negative charges were neutralized by cytochrome *C* for both types of nanoparticles. In the case of polymer blend nanoparticles, the ζ-potential increased gradually as the concentration of cytochrome *C* increased, leveling off at −18 mV at 300 μg/ml. In contrast, for PLGA nanoparticles, the ζ-potential increased more sharply at lower concentrations of cytochrome *C*, and was already near the plateau value at 150 μg/ml, indicating a faster neutralization of surface charge. Upon comparing Fig. 9a and b, one can see that due to the higher surface charge density on the PLGA/PSS particles compared to PLGA particles, more cytochrome *C* is required to neutralize the charge on the former.

Negligible changes in size were observed for PLGA/PSS nanoparticles ($P > 0.05$) after incubation with cytochrome *C*. In contrast, flocculation occurred with the PLGA nanoparticles at protein concentrations of 200–250 μg/ml, and aggregates were observed upon incubation with 300–400 μg/ml cytochrome *C*. The reduced net charge on the surface and the accompanying reduction in repulsive forces between the particles led to this aggregation.

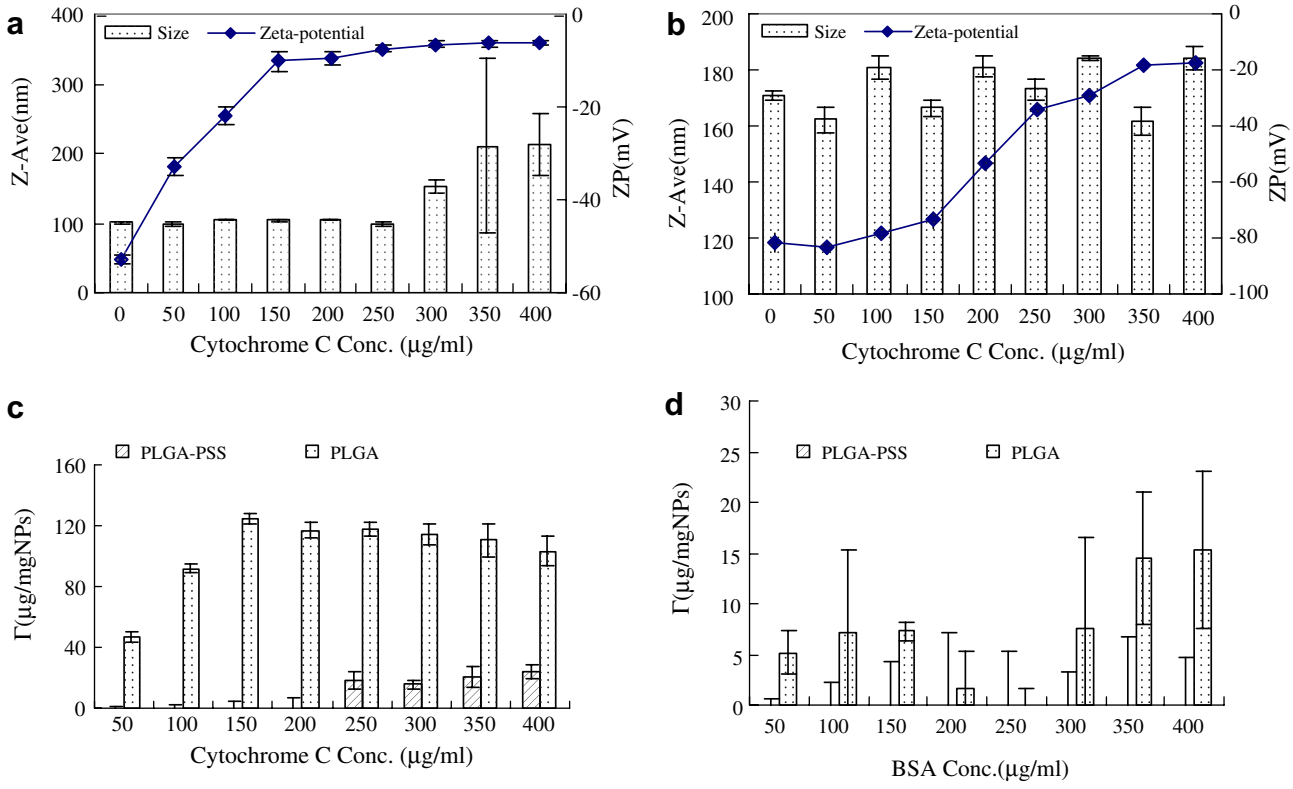

Fig. 9. Size (Z-Ave) and ζ-potential (ZP) of PLGA (a) or PLGA/PSS (b) nanoparticles after incubation with cytochrome *C*. Loading capacity (Γ) of cytochrome *C* (c) and BSA (d) to PLGA and PLGA/PSS nanoparticles ($n = 3$).

Previous studies have reported the complexation of cytochrome *C* with sulfonated polystyrene nanoparticles through electrostatic interactions [34,35]. Surprisingly, in this work, as indicated in Fig. 9c, the maximum amount of cytochrome *C* adsorbed is lower for the PLGA/PSS nanoparticles (24 μg/mg) than for the PLGA nanoparticles (103 μg/ml), even though the PLGA/PSS nanoparticles carried more net negative charge. Therefore, it can be deduced that the interaction of lysozyme with PLGA/PSS nanocarriers is highly affected by the surface charge [36], but for cytochrome *C*, the electrostatic interaction is not the primary driving force for adsorption. Bayraktar et al. [37] suggest that facial specificity for nanoparticle binding is apparently determined by a fine balance between electrostatics and hydrophobicity; for cytochrome *C*, a combination of hydrophobic and coulombic interactions would lead to better binding efficiency. Rezwan et al. also suggest that electrostatic interactions seem to govern protein adsorption in the cases where the protein and material surfaces are very hydrophilic [38].

After incubation of both types of nanoparticles with BSA, no noticeable aggregates nor obvious changes in ζ-potential were observed at any of the BSA concentrations studied. No adsorption of BSA was achieved for PLGA/PSS particles, but a small amount of BSA (about 15 μg/mg) was adsorbed to the PLGA particles (see Fig. 9d). It has been previously reported that proteins can overcome repulsive electrostatic interactions and still adsorb [28], but this adsorption is not as effective as observed near the isoelectric point or at a pH which allows for opposite (attractive) charges. These results suggest that electrostatics play a dominant role in driving adsorption, but additional non-coulombic factors such as London, van der Waals, and hydrophobic forces also play a role.

In the previously mentioned report concerning slightly sulfonated polystyrene particles [34], the ionic groups on the particle surface stabilize the hydrophobic core of polystyrene chains. It can be deduced by analogy that for the PLGA/PSS particles in this work, the higher density of sulfonate functional groups on the surface leads to more hydrophilicity than exhibited by the pure PLGA particles. For this reason, the PLGA particles are able to participate in more hydrophobic interactions in the adsorption process, and, in the case of BSA adsorption, overcome electrostatic repulsion.

3.5. Release and bioactivity

In vitro experiments monitoring the release of lysozyme from nanoparticles at different theoretical drug loadings were performed in pH 7.4 PBS. During these experiments, the stability of the lysozyme solution was investigated as control. No significant differences ($p > 0.05$) were observed in lysozyme concentrations at each time point during the release process as measured by both BCA assay and bioactivity, which indicates that the sampling process had no effect on lysozyme bioactivity.

Fig. 10 shows the release of lysozyme from three different nanoparticle formulations. It can be seen that the release rate of protein from PLGA/PSS nanoparticles at 10% loading was much faster than that at 40% loading. The increased amount of protein loaded decreased the release rate. As this release process is mainly a combination of desorption and diffusion process, possible explanation of these results is that the increased amount of lysozyme in the 40% loading sample enhanced the interaction between the protein and the nanoparticles, which led to the slower release. In addition, the coating of protein adsorbed to the nanoparticle surface can decrease the diffusion of protein by reducing the porosity or decreasing the swelling of the nanoparticles. This dependence of release on loading amount is in agreement with a previous report [39], in which chloroquine phosphate was loaded onto gelatin nanoparticles through similar adsorption method and also released faster at a lower drug loading.

The release of lysozyme from the 5%-loaded RG502H nanoparticles is slower than the 10%-loaded polymer blend particles. This probably reflects the differences in the protein-particle interaction mechanisms. Hydrophobic forces play a more important role for the PLGA particles than for the PLGA/PSS nanoparticles, and the release rate from the PLGA particles can be attributed to these hydrophobic interactions. In contrast, electrostatic interactions between the hydrophilic surface of the polymer blend nanoparticles and lysozyme are of more importance for the PLGA/PSS system.

In order to verify that the particle preparation and release process do not denature the protein, the bioactivity of released lysozyme was determined. Fig. 11 shows the concentration and bioactivity of lysozyme released from 40%-loaded nanoparticles. There were no significant differences between the two measures at any of the time points ($P > 0.05$), which confirms that no lysozyme denaturation was detected during the process of adsorption onto the

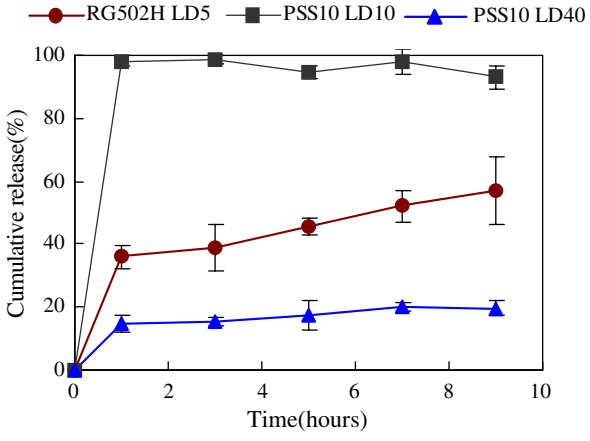

Fig. 10. In vitro release profiles of lysozyme from PLGA and PLGA/PSS nanoparticles at different theoretical drug loading values. RG502H LD5: PLGA nanoparticles with theoretical drug loading of 5%; PSS10LD10 and PSS10LD40: PLGA/PSS nanoparticles at a ratio of 10% of PSS to PLGA, with theoretical drug loadings of 10% and 40%, respectively. Each data point represents mean ± standard deviation ($n = 3$).

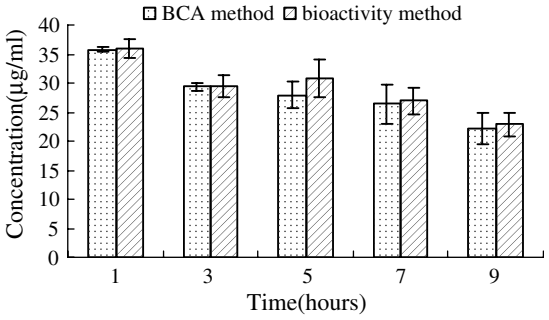

Fig. 11. Comparison of the concentrations and bioactivity of lysozyme released from PLGA/PSS nanoparticles (10% PSS, 40% theoretical protein loading), as measured by BCA assay and activity against *Micrococcus lysodeikticus* cell walls, respectively ($n = 3$).

nanoparticles or during the release. Based on these data, it may be concluded that this is a facile and feasible method for preparing protein-loaded nanoparticles.

4. Conclusions

In the present report we describe the feasibility of employing a model negatively charged nanocarrier system, consisting of a polymer blend of PLGA and PSS, for increasing the loading capacity of the model positively charged protein lysozyme based on the increased negative charge density of the nanoparticles. Investigations of pH and ionic strength suggest that electrostatic interactions primarily govern the adsorption process, but that hydrophobic interactions also play a minor role. Moreover, the adsorption behavior of cytochrome *C* showed different adsorption mechanism that a fine balance of hydrophobic and electrostatic interaction is required for efficient adsorption. The study of BSA adsorption highlighted the importance of hydrophobic interactions between protein and nanoparticles for efficient loading. The lower adsorption capacity of BSA compared to cytochrome *C* and lysozyme indicated the importance of electrostatic interaction for adsorption process. The release rate of lysozyme from nanoparticles was dependent on drug loading, and the preservation of full protein bioactivity was demonstrated. Taken together, our results suggest a feasible method to improve the loading capacity of proteins based on the electrostatic interactions between oppositely charged proteins and nanoparticles. Further studies involving new types of negatively charged polymers recently developed in our research group are currently in progress.

Acknowledgments

Cuifang Cai would like to acknowledge the German Academic Exchange Service (Deutsche Akademische Austauschdienst, DAAD) for the financial support. We thank Johannes Sitterberg for the AFM images, and Michael Hellwig for his assistance about TEM and SEM images.

References

[1] J. Panyam, V. Labhasetwar, Biodegradable nanoparticles for drug and gene delivery to cells and tissue, Adv. Drug Deliv. Rev. 55 (2003) 329–347.
[2] K.S. Soppimath, T.M. Aminabhavi, A.R. Kulkarni, W.E. Rudzinski, Biodegradable polymeric nanoparticles as drug delivery devices, J. Control. Release 70 (2001) 1–20.
[3] A. Brunner, K. Maeder, A. Goepferich, pH and osmotic pressure inside biodegradable microspheres during erosion, Pharm. Res. 16 (1999) 847–853.
[4] T. Jung, A. Breitenbach, T. Kissel, Sulfobutylated poly(vinyl alcohol)-graft-poly(lactide-co-glycolide)s facilitate the preparation of small negatively charged biodegradable nanospheres, J. Control. Release 67 (2000) 157–169.
[5] M.C. Julienne, M.J. Alonso, J.L. Gomez Amoza, J.P. Benoit, Preparation of poly(DL-lactide/glycolide) nanoparticles of controlled particle size distribution: application of experimental designs, Drug Dev. Ind. Pharm. 18 (1992) 1063–1077.
[6] P. Couvreur, B. Kante, M. Roland, P. Guiot, P. Bauduin, P. Speiser, Polycyanoacrylate nanocapsules as potential lysosomotropic carriers: preparation, morphological and sorptive properties, J. Pharm. Pharmacol. 31 (1979) 331–332.
[7] E. Allemann, J.C. Leroux, R. Gurny, E. Doelker, In vitro extended-release properties of drug-loaded poly(DL-lactic acid) nanoparticles produced by a salting-out procedure, Pharm. Res. 10 (1993) 1732–1737.
[8] H. Fessi, F. Puisieux, J.P. Devissaguet, N. Ammoury, S. Benita, Nanocapsule formation by interfacial polymer deposition following solvent displacement, Int. J. Pharm. 55 (1989) R1–R4.
[9] C.V. Sternling, L.E. Scriven, Interfacial turbulence: hydrodynamic instability and the Marangoni effect, AIChE J. 5 (1959) 514–523.
[10] B. Dimitrova, I. Ivanov, E. Nakache, Mass transport effects on the stability of emulsion: emulsion films with acetic acid and acetone diffusing across the interface, J. Dispers. Sci. Technol. 9 (1988) 321–341.
[11] J.A. Schrier, P.P. DeLuca, Porous bone morphogenetic protein-2 microspheres: polymer binding and in vitro release, AAPS Pharm. Sci. Technol. 2 (2001) E17.
[12] T. Niwa, H. Takeuchi, T. Hino, N. Kunou, Y. Kawashima, Preparations of biodegradable nanospheres of water-soluble and insoluble drugs with DL-lactide/glycolide copolymer by a novel spontaneous emulsification solvent diffusion method, and the drug release behavior, J. Control. Release 25 (1993) 89–98.
[13] T. Jung, W. Kamm, A. Breitenbach, G. Klebe, T. Kissel, Loading of tetanus toxoid to biodegradable nanoparticles from branched poly(sulfobutyl-polyvinyl alcohol)-g-(lactide-co-glycolide) nanoparticles by protein adsorption: a mechanistic study, Pharm. Res. 19 (2002) 1105–1113.
[14] X. Li, Y. Zhang, R. Yan, W. Jia, M. Yuan, X. Deng, Z. Huang, Influence of process parameters on the protein stability encapsulated in poly-DL-lactide-poly(ethylene glycol) microspheres, J. Control. Release 68 (2000) 41–52.
[15] W. Lu, T.G. Park, Protein release from poly(lactic-co-glycolic acid) microspheres: protein stability problems, PDA J. Pharm. Sci. Technol. 49 (1995) 13–19.
[16] K. Rezwan, L.P. Meier, L.J. Gauckler, Lysozyme and bovine serum albumin adsorption on uncoated silica and AlOOH-coated silica particles: the influence of positively and negatively charged oxide surface coatings, Biomaterials 26 (2005) 4351–4357.
[17] T. Jung, W. Kamm, A. Breitenbach, K.D. Hungerer, E. Hundt, T. Kissel, Tetanus toxoid loaded nanoparticles from sulfobutylated poly(vinyl alcohol)-graft-poly(lactide-co-glycolide): evaluation of antibody response after oral and nasal application in mice, Pharm. Res. 18 (2001) 352–360.
[18] R. Ghaderi, J. Carlfors, Biological activity of lysozyme after entrapment in poly(d,l-lactide-co-glycolide)-microspheres, Pharm. Res. 14 (1997) 1556–1562.

[19] M. Van de Weert, J. Hoechstetter, W.E. Hennink, D.J. Crommelin, The effect of a water/organic solvent interface on the structural stability of lysozyme, J. Control. Release 68 (2000) 351–359.
[20] A. Wittemann, M. Ballauff, Secondary structure analysis of proteins embedded in spherical polyelectrolyte brushes by FT-IR spectroscopy, Anal. Chem. 76 (2004) 2813–2819.
[21] C. Czeslik, R. Jansen, M. Ballauff, A. Wittemann, C.A. Royer, E. Gratton, T. Hazlett, Mechanism of protein binding to spherical polyelectrolyte brushes studied in situ using two-photon excitation fluorescence fluctuation spectroscopy, Phys. Rev. E 69 (2004) 021401.
[22] S. Rosenfeldt, A. Wittemann, M. Ballauff, E. Breininger, J. Bolze, N. Dingenouts, Interaction of proteins with spherical polyelectrolyte brushes in solution as studied by small-angle X-ray scattering, Phys. Rev. E 70 (2004) 061403.
[23] B. Haupt, T. Neumann, A. Wittemann, M. Ballauff, Activity of enzymes immobilized in colloidal spherical polyelectrolyte brushes, Biomacromolecules 6 (2005) 948–955.
[24] P.M. Biesheuvel, A. Wittemann, A modified box model including charge regulation for protein adsorption in a spherical polyelectrolyte brush, J. Phys. Chem. B 109 (2005) 4209–4214.
[25] K. Anikin, C. Rocker, A. Wittemann, J. Wiedenmann, M. Ballauff, G.U. Nienhaus, Polyelectrolyte-mediated protein adsorption: fluorescent protein binding to individual polyelectrolyte nanospheres, J. Phys. Chem. B 109 (2005) 5418–5420.
[26] W. Norde, J. Lyklema, The adsorption of human plasma albumin bovine pancreas ribonuclease at negatively charged polystyrene surfaces. II. Hydrogen ion titrations, J. Coll. Interf. Sci. 66 (1978) 266–276.
[27] W. Norde, J. Lyklema, The adsorption of human plasma albumin and bovine pancreas ribonuclease at negatively charged polystyrene surfaces. I. Adsorption isotherms. Effects of charge, ionic strength, and temperature, J. Coll. Interf. Sci. 66 (1978) 257–265.
[28] J. Chesko, J. Kazzaz, M. Ugozzoli, T. O'Hagan D, M. Singh, An investigation of the factors controlling the adsorption of protein antigens to anionic PLG microparticles, J. Pharm. Sci. 94 (2005) 2510–2519.
[29] K. Rezwan, L.P. Meier, L.J. Gauckler, A prediction method for the isoelectric point of binary protein mixtures of bovine serum albumin and lysozyme adsorbed on colloidal titania and alumina particles, Langmuir 21 (2005) 3493–3497.
[30] P.M. Biesheuvel, P. Stroeve, P.A. Barneveld, Effect of protein adsorption and ionic strength on the equilibrium partition coefficient of ionizable macromolecules in charged nanopores, J. Phys. Chem. B 108 (2004) 17660–17665.
[31] Y.C. Liu, E. Stellwagen, Accessibility and multivalency of immobilized Cibacron blue F3GA, J. Biol. Chem. 262 (1987) 583–588.
[32] S. Robinson, P.A. Williams, Inhibition of protein adsorption onto silica by polyvinylpyrrolidone, Langmuir 18 (2002) 8743–8748.
[33] S. Zhang, Y. Sun, Further studies on the contribution of electrostatic and hydrophobic interactions to protein adsorption on dye-ligand adsorbents, Biotechnol. Bioeng. 75 (2001) 710–717.
[34] J. Gong, P. Yao, H. Duan, M. Jiang, S. Gu, L. Chunyu, Structural transformation of cytochrome *c* and Apo cytochrome *c* induced by sulfonated polystyrene, Biomacromolecules 4 (2003) 1293–1300.
[35] L. Liang, P. Yao, J. Gong, M. Jiang, Interaction of apo cytochrome *c* with sulfonated polystyrene nanoparticles, Langmuir 20 (2004) 3333–3338.
[36] P. Calvo, J.L. Vila-Jato, M.J. Alonso, Effect of lysozyme on the stability of polyester nanocapsules and nanoparticles: stabilization approaches, Biomaterials 18 (1997) 1305–1310.
[37] H. Bayraktar, C.-C. You, V.M. Rotello, M.J. Knapp, Facial control of nanoparticle binding to cytochrome *c*, J. Am. Chem. Soc. 129 (2007) 2732–2733.
[38] K. Rezwan, A.R. Studart, J. Voros, L.J. Gauckler, Change of zeta potential of biocompatible colloidal oxide particles upon adsorption of bovine serum albumin and lysozyme, J. Phys. Chem. B 109 (2005) 14469–14474.
[39] F.Q. Hu, G.F. Ren, H. Yuan, Y.Z. Du, S. Zeng, Shell cross-linked stearic acid grafted chitosan oligosaccharide self-aggregated micelles for controlled release of paclitaxel, Coll. Surf. B 50 (2006) 97–103.